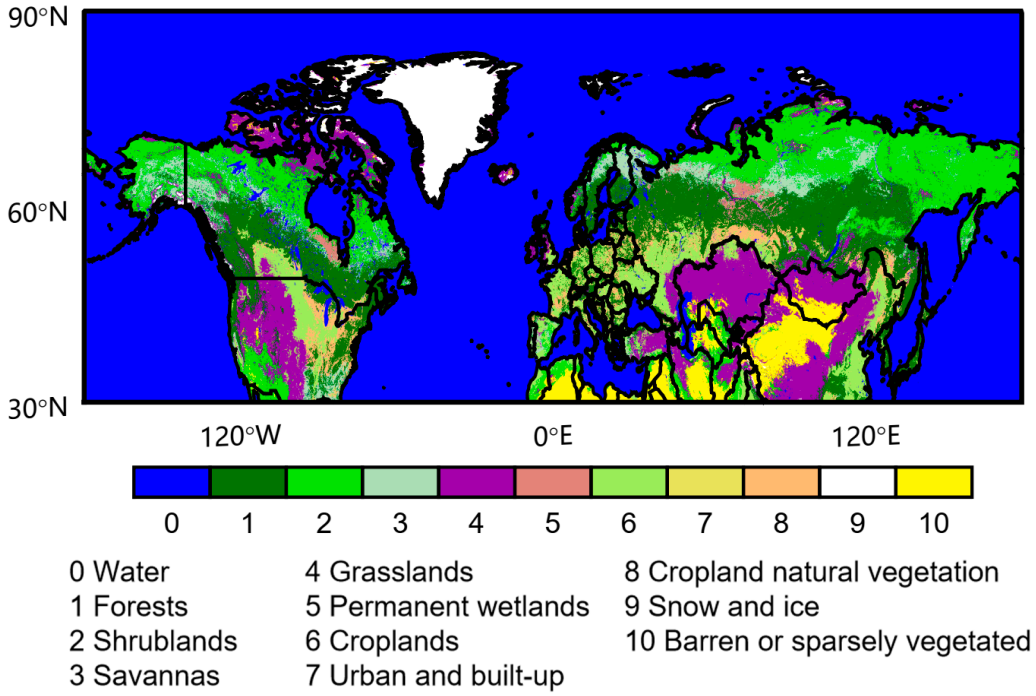

Figure S1. Spatial distributions of the different land cover types based on MODIS data for the Northern Hemisphere.

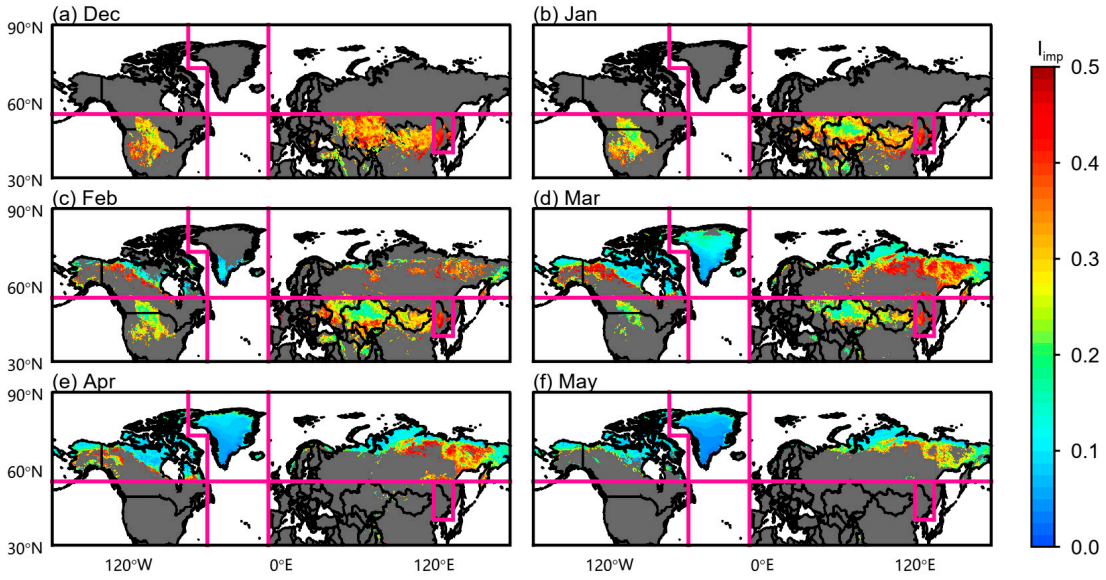

Figure S2. Spatial distributions of averaged multi-year (2003–2018) I_{imp} for (a) December, (b) January, (c) February, (d) March, (e) April, and (f) May.

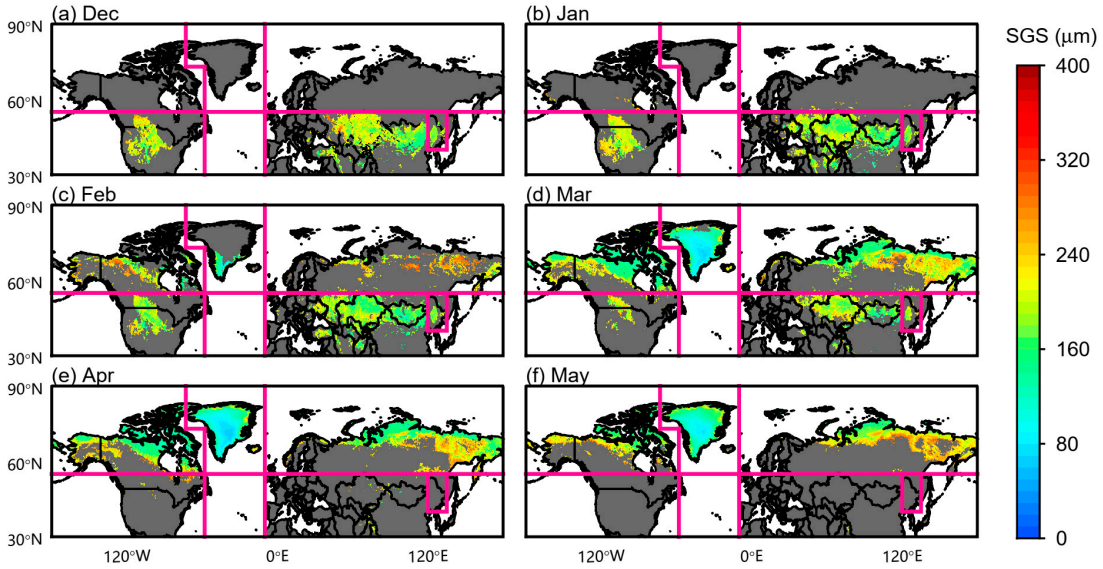

Figure S3. Spatial distributions of averaged multi-year (2003–2018) SGS for (a) December, (b) January, (c) February, (d) March, (e) April, and (f) May.

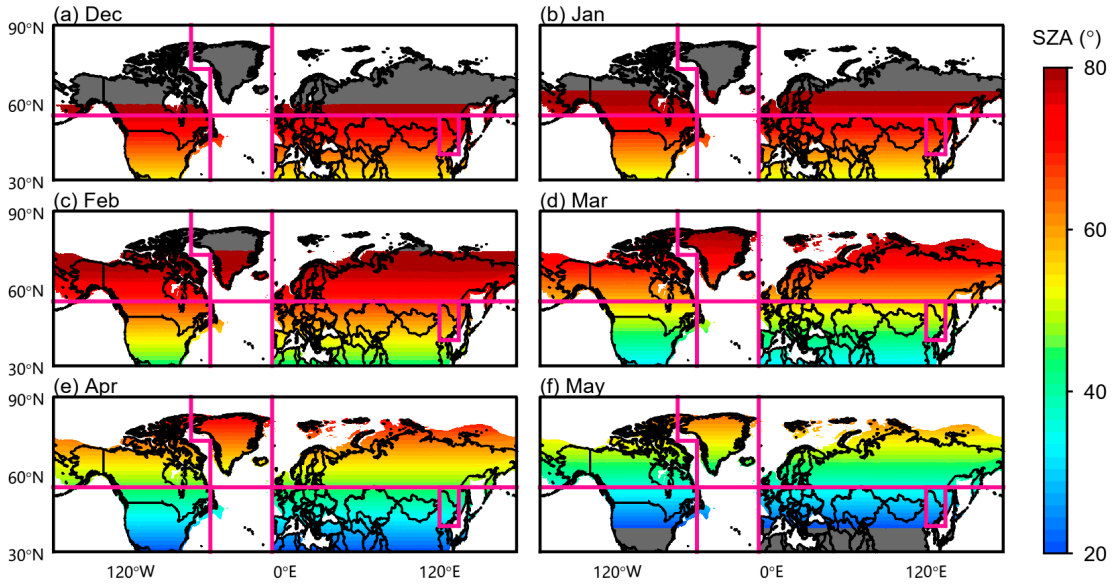

Figure S4. Spatial distributions of averaged multi-year (2003–2018) SZA for (a) December, (b) January, (c) February, (d) March, (e) April, and (f) May.

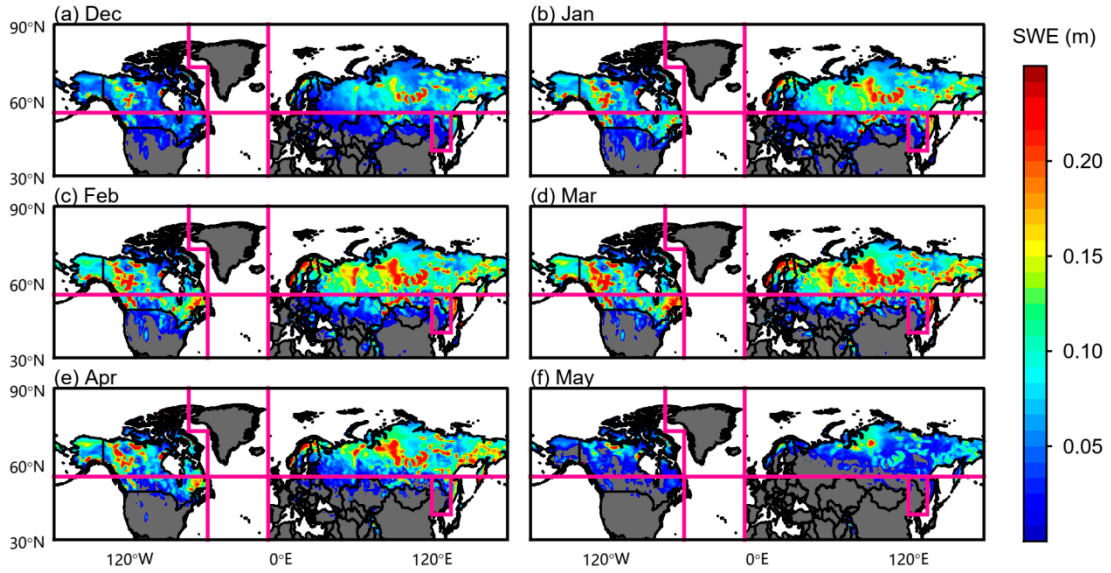

Figure S5. Spatial distributions of averaged multi-year (2003–2018) SWE for (a) December, (b) January, (c) February, (d) March, (e) April, and (f) May.

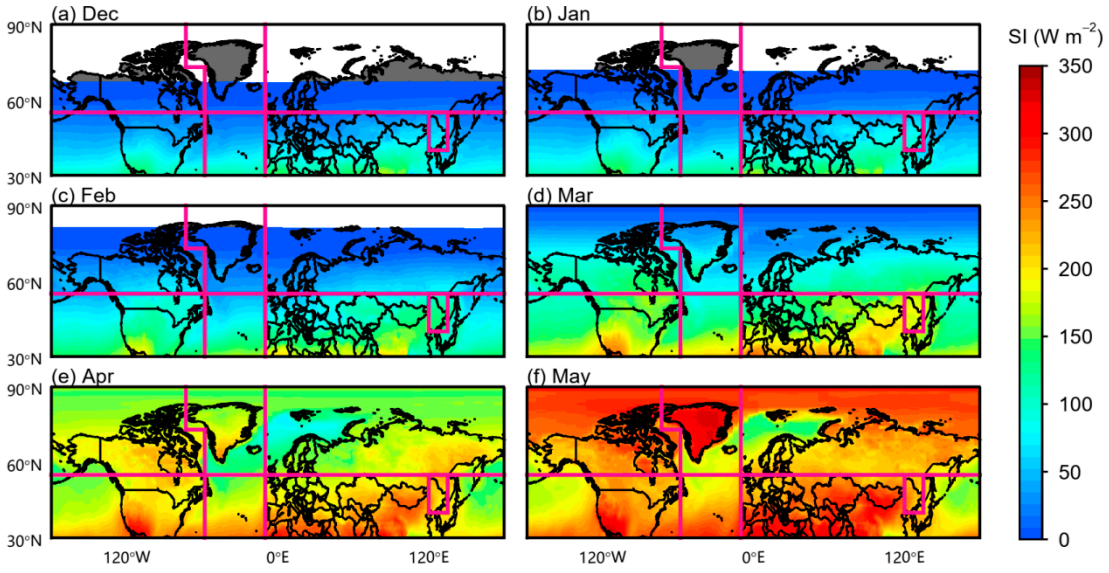

Figure S6. Spatial distributions of averaged multi-year (2003–2018) SI for (a) December, (b) January, (c) February, (d) March, (e) April, and (f) May.

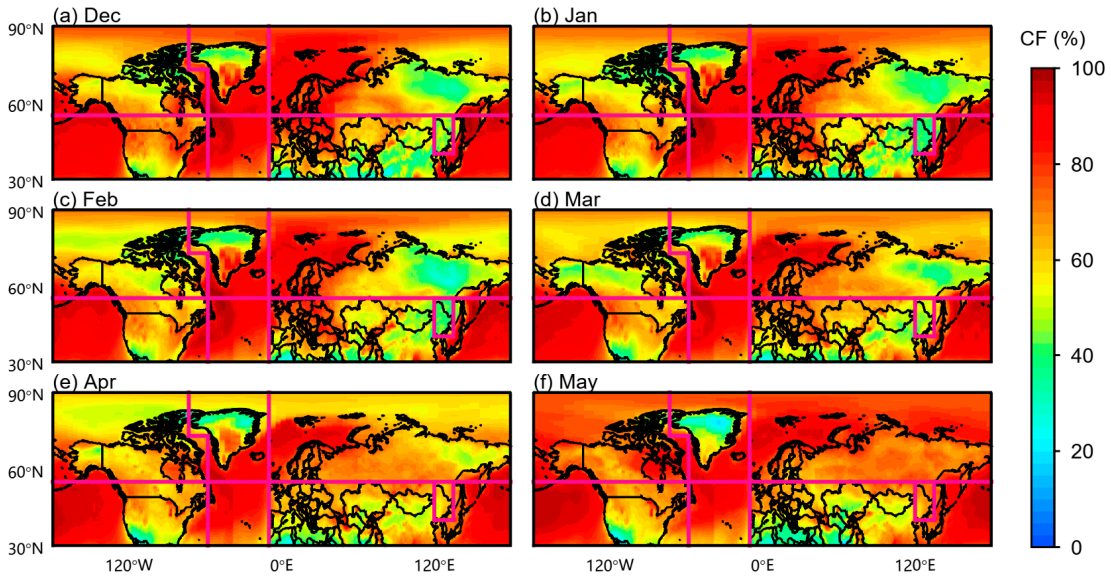

Figure S7. Spatial distributions of averaged multi-year (2003–2018) CF for (a) December, (b) January, (c) February, (d) March, (e) April, and (f) May.

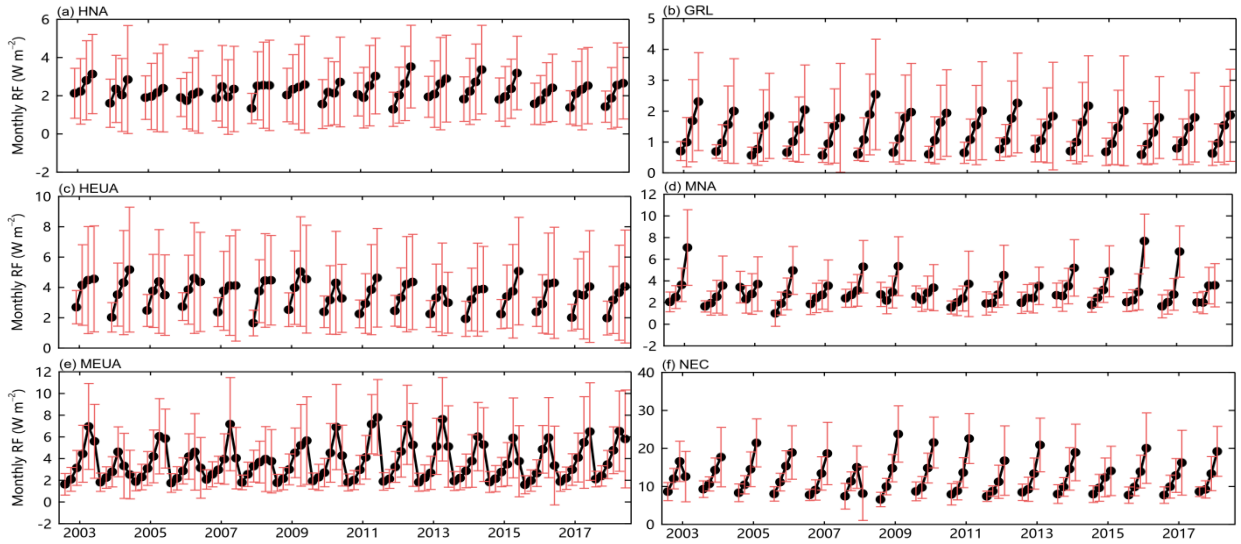

Figure S8. Monthly radiative forcing for each region during the period 2003–2018.

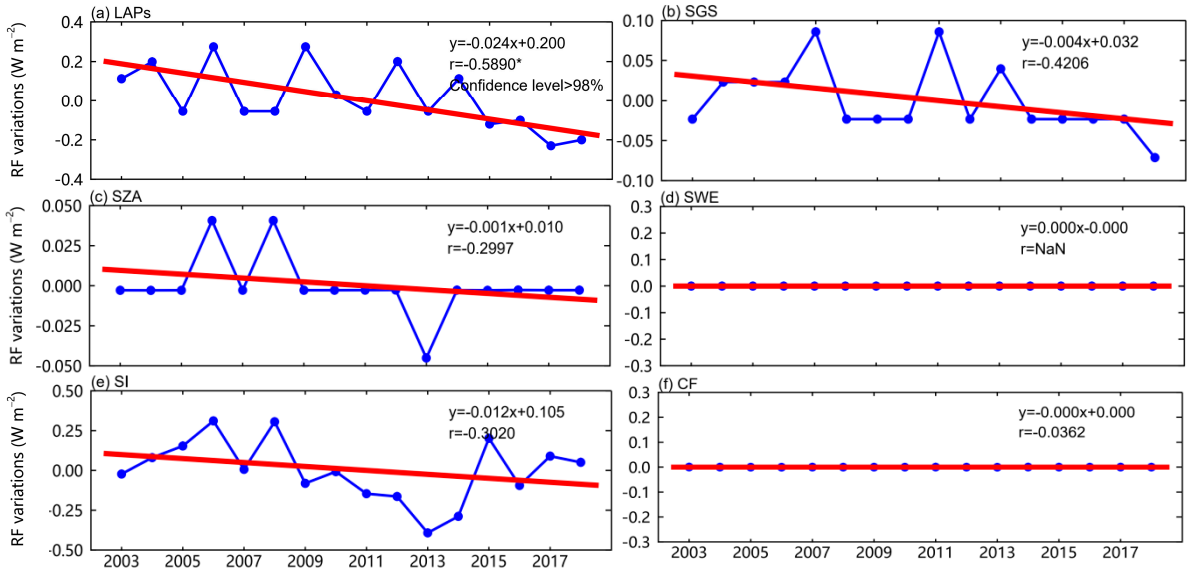

Figure S9. RF variations in HUEA due to each forcing factor.

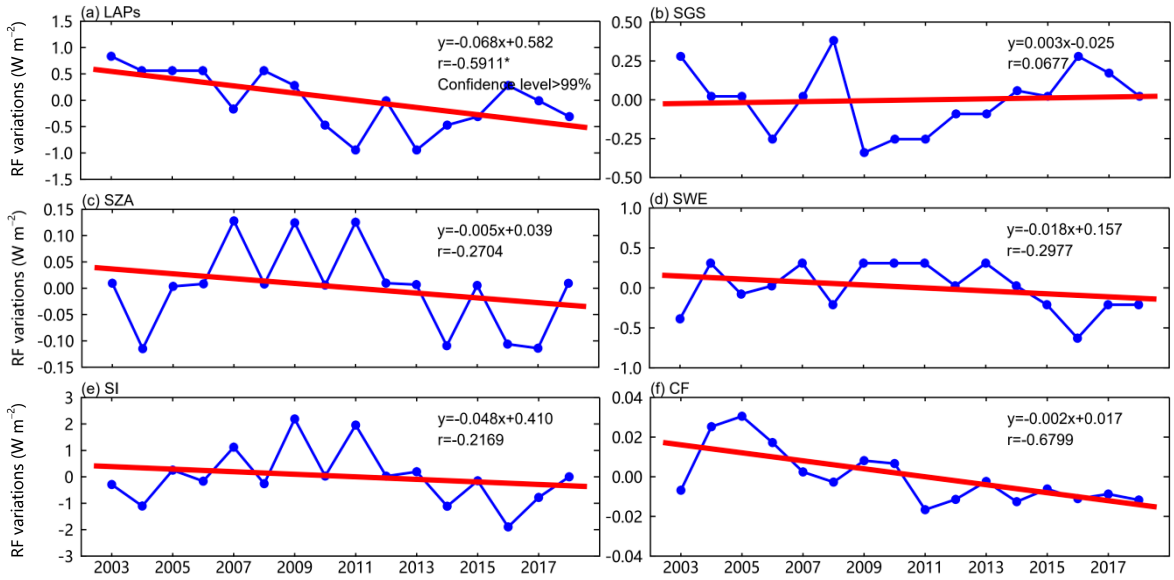

Figure S10. RF variations in NEC due to each forcing factor.